Individual differences in beta frequency correlate with the audio-visual fusion illusion

Noguchi, Yasuki

(Citation)
Psychophysiology,59(8):e14041

(Issue Date)
2022-08-01

(Resource Type)
journal article

(Version)
Accepted Manuscript

Individual differences in beta frequency correlate with the audio–visual fusion illusion

Yasuki Noguchi

Department of Psychology, Graduate School of Humanities, Kobe University, 1-1 Rokkodai-cho, Nada, Kobe, 657-8501, Japan.

Correspondence
Yasuki Noguchi, Department of Psychology, Kobe University, 1-1 Rokkodai-cho, Nada, Kobe, 657-8501, Japan. Tel. +1-78-803-5516, E-mail: ynoguchi@lit.kobe-u.ac.jp

Short title: Separate neural cycles for AV fission and fusion

Number of figures: 6 in the main document and 4 in the Supporting Information (no tables)

Abstract

Presenting one flash with two beeps induces a perception of two flashes (audio–visual fission illusion), while presenting two flashes with one beep induces a perception of one flash (fusion illusion). Although previous studies showed a relationship between the frequency of the alpha rhythm (alpha cycle) and one's susceptibility to the fission illusion, the relationship between neural oscillations and the fusion illusion is unknown. Using electroencephalography, here I investigated the frequency of oscillatory signals in the pre-stimulus period and found a significant correlation between the beta rhythm and the fusion illusion; specifically, participants with a lower beta frequency showed a larger fusion illusion. These data indicate two separate time windows of audio–visual integration in the human brain, one defined by the alpha cycle (fission) and another defined by the beta cycle (fusion).

KEYWORDS: electroencephalography; alpha frequency; beta frequency; sound-induced flash illusion

1. INTRODUCTION

We live in a world characterized by multiple sources of sensory information. The ability to combine sensory inputs across different modalities is a key function for accurately perceiving our environments (Hirst, McGovern, Setti, Shams, & Newell, 2020; Keil, 2020; Rohe, Ehlis, & Noppeney, 2019; Zhou, Cheung, & Chan, 2020). In particular, the integration of visual and auditory stimuli plays a critical role in many cognitive processes, such as language (Conrey & Pisoni, 2006; Francisco, Jesse, Groen, & McQueen, 2017; Gogate, Walker-Andrews, & Bahrick, 2001; Kaganovich, 2017; Lewkowicz, Leo, & Simion, 2010), emotion processing (WalkerAndrews, 1997), and social recognition (Noel, De Niear, Lazzara, & Wallace, 2018; Robertson & Schweinberger, 2010; Stevenson et al., 2016; Woynaroski et al., 2013).

The sound-induced flash illusion (SIFI) (Shams, Kamitani, & Shimojo, 2000) is one of the most famous phenomena resulting from the integration of visual and auditory inputs. When a single visual stimulus (flash) is presented simultaneously with two auditory stimuli (beeps), people often report a perception of two flashes (fission illusion). Conversely, presenting two flashes with one beep results in the perception of one flash (fusion illusion) (Andersen, Tiippana, & Sams, 2004).

An open question in this classical paradigm is whether the fission and fusion illusions arise from the same neural mechanism (Apthorp, Alais, & Boenke, 2013; Hirst et al., 2020; McGovern, Roudaia, Stapleton, McGinnity, & Newell, 2014). Many previous models of the SIFI propose that the brain makes perceptual decisions by weighing sensory information according to its relative reliability (Alais & Burr, 2004; Ernst & Bulthoff, 2004). Therefore, vision tends to dominate in spatial judgments because of its higher spatial resolution, while audition dominates in temporal judgments. These models suggest that fission and fusion illusions emerge from a common mechanism, namely the higher temporal resolution of audition than vision. This view was supported by an empirical study (Apthorp et al., 2013) that investigated changes in the magnitude of the fission/fusion illusion as a function of stimulus-onset asynchrony between two beeps/flashes. The time course of fission was similar to that of fusion, suggesting a common mechanism of these two illusions.

On the other hand, several recent studies have provided behavioral data indicating a separation of the fusion and fission illusions (Abadi & Murphy, 2014; DeLoss & Andersen, 2015; Kostaki & Vatakis, 2016; Wang et al., 2019). For example, older adults were more susceptible to the fission illusion than younger participants, while the magnitude of the fusion illusion was almost identical between the two groups (McGovern et al., 2014). Adults with autism spectrum disorder and typically developing individuals showed similar performances

in the fission illusion but not in the fusion illusion (Bao, Doobay, Mottron, Collignon, & Bertone, 2017).

In this study, I used electroencephalography (EEG) and investigated possible differences between the two illusions by analyzing neural oscillation cycles in the brain. Previous studies have shown that individuals with a lower alpha rhythm frequency during a baseline (pre-stimulus) period showed a larger fission illusion (Cecere, Rees, & Romei, 2015; Cooke, Poch, Gillmeister, Costantini, & Romei, 2019; Keil & Senkowski, 2017; Venskus & Hughes, 2021). This suggests that the alpha cycle (around 100 ms) represents the temporal window for the integration of visual and auditory inputs. I hypothesized that if the fission and fusion illusions reflect different neural mechanisms, they can be separated in a frequency domain. Specifically, the magnitude of the fusion illusion might be correlated with an oscillation frequency other than alpha waves, such as the delta (1–4 Hz), theta (4–8 Hz), beta (13–30 Hz), or gamma (> 30 Hz) rhythm.

2. METHOD

2.1 Participants

Twenty-nine healthy participants (age: 18–42 years, 17 females) took part in the study. Data of two participants (females) were discarded because of excessive noise in EEG waveforms, and were replaced by the data of two additional participants (females). This sample size (29) was determined by a power analysis using G*Power 3 (Faul, Erdfelder, Lang, & Buchner, 2007). The type I error rate and statistical power were set at 0.05 and 0.80, respectively. The effect size was assumed to be large (r = 0.5) based on previous studies reporting a strong correlation between the alpha cycle and the fission illusion (Cecere et al., 2015; Cooke et al., 2019). The nature of the study was explained to each participant and informed consent was then obtained. All experiments conformed to the guidelines and regulations of the ethics committee at Kobe University, Japan.

2.2 Stimuli and task

All visual and auditory stimuli were generated using Matlab Psychophysics Toolbox (Brainard, 1997; Pelli, 1997) and were presented on a CRT monitor (refresh rate: 60 Hz) or by two speakers (intensity: 77 dB SPL), with one each on either side of the CRT monitor. As shown in **Figure 1A**, each trial started with presentation of a blank screen (0.01 cd/m^2) for 500 ms, followed by a fixation period of 500–600 ms. The size of the red fixation point was 0.18° × 0.18°. A varying number of flashes (0–2) were then synchronized with a varying

number of beeps (0–2). The position of each flash (a white circle with a diameter of 4.69°, luminance: 55 cd/m^2, duration: 1 frame of the CRT monitor) was either 12.5° left or right of the fixation point. The beep was a pure tone (4,000 Hz) of 8 ms with 1-ms rise and fall times. In both visual and auditory modalities, the stimulus onset asynchrony (SOA) between two successive stimuli was set at 50 ms (**Fig. 1B**). One second after the onset of the first flash or first beep, a task screen was displayed asking participants to report the perceived number of flashes (0, 1, or 2), ignoring all beeps. No time limit was imposed. The next trial started after a rest screen (300 ms) informing how many trials the participants had completed.

Combinations of 0–2 flashes with 0–2 beeps resulted in eight types of trials, as shown in **Figure 1C**. A flash and a beep were simultaneously presented in 1F1B trials, while 2F2B trials had two flashes synchronized with two beeps. The fission and fusion illusions were induced in 1F2B and 2F1B trials, respectively. Flash-only (1F0B and 2F0B) and beep-only (1B and 2B) trials were also employed to serve as baselines (see below).

An experimental session comprised 126 trials in which the eight types of trials were randomly intermixed (the number of trials for each condition is shown in **Fig. 1C**). In the left-flash (LF) session, all flashes were shown in the left visual field, while they were shown in the right visual field in the right-flash (RF) session. An entire experiment consisted of six sessions (three LF and three RF), with the order of LF and RF sessions randomized across participants.

2.3. Analysis of behavioral data

Consistent with previous studies (Apthorp et al., 2013; Bolognini et al., 2016; Narinesingh, Goltz, & Wong, 2017), the magnitudes of the fission and fusion illusions were quantified as changes in task accuracy from baseline (no-beep) conditions. Specifically, the magnitude of the fission illusion was measured as the decrease in accuracy from the 1F0B to the 1F2B condition, while that of the fusion illusion was assessed as the decrease from the 2F0B to the 2F1B condition (**Fig. 2A**).

To disentangle perceptual sensitivity (*d'*) from response criteria (ln(β)), the magnitude of the fusion illusion was also quantified based on signal detection theory (Keil, 2020; Vanes et al., 2016; Watkins, Shams, Tanaka, Haynes, & Rees, 2006) (see **RESULTS** and **Fig. 6**). In this approach, the hit rate of the fusion illusion was defined as the proportion of trials that participants reported "1 flash" in 1F1B trials, while the false-alarm (FA) rate was the probability of reporting "1 flash" in 2F1B trials. Perceptual sensitivity (*d'*) was computed using the equation

$d' = z(\text{hit rate}) - z(\text{FA rate})$,

where z indicates the inverse cumulative normal function. A larger-magnitude fusion illusion was indexed by a higher FA rate and smaller d'. On the other hand, the response criterion (ln(β)) was estimated as

$$\ln(\beta) = [z(\text{FA rate})^2 - z(\text{hit rate})^2]/2.$$

A positive ln(β) indicates a tendency (response bias) toward reporting "2 flashes" in all types of trials.

I also computed d' and ln(β) for fission illusion and correlated them with oscillatory cycles in **Figure S4**. The hit rate was defined as the proportion of reporting "2 flashes" in 2F2B trials, while the FA rate was the probability of reporting "2 flashes" in 1F2B trials.

2.4 EEG measurements and analyses

EEG signals were measured at 32 points on the scalp (FP1, FP2, AF3, AF4, F7, F3, Fz, F4, F8, FC5, FC1, FC2, FC6, T7, C3, Cz, C4, T8, CP5, CP1, CP2, CP6, P7, P3, Pz, P4, P8, PO3, PO4, O1, Oz, and O2, see **Fig. 3A**). Measurements were carried out with an ActiveTwo EEG system (Biosemi, Amsterdam, Netherlands) at a sampling rate of 2,048 Hz and an analog low-pass filter of 417 Hz. Using the Brainstorm toolbox for Matlab (Tadel, Baillet, Mosher, Pantazis, & Leahy, 2011), all data were re-referenced with an average potential over the 32 sensors. Artifacts and noise were corrected by a digital band-pass filter of 0.5–200 Hz (Butterworth, 4th order). EEG waveforms in the pre-stimulus period (from −1,000 to 0 ms relative to the onset of the first flash or beep) were then segmented and converted into power spectral density (PSD) with Welch's method. I defined six frequency bands (delta: 1–4 Hz, theta: 4–8 Hz, alpha: 8–13 Hz, beta: 13–30 Hz, gamma: 31–58 Hz, and high gamma: 62–100 Hz), avoiding power-line noise at 60 Hz. The central frequency of each band was calculated as the weighted mean of frequencies × powers (Klimesch, Schimke, & Pfurtscheller, 1993; Samuel, Wang, Hu, & Ding, 2018). For example, the central alpha frequency (Hz) was obtained using the formula below:

$$\text{Central alpha frequency} = \frac{\sum_{f=8}^{13} power(f) \times f}{\sum_{f=8}^{13} power(f)},$$

where f indicates the component frequencies in the alpha band (8–13 Hz) and *power(f)* indicates the powers of these frequencies on the PSD. The cycle of oscillatory signals was

estimated as the inverse of the central frequency averaged across all 756 trials (e.g., the alpha cycle was 100 ms when the participant's central alpha frequency was 10 Hz).

An alternative method for measuring oscillation frequency is to directly search for the component frequency with a maximum power on PSD (Cecere et al., 2015; Cooke et al., 2019; Venskus & Hughes, 2021). The results of this analysis (peak-frequency analysis) are shown in **Supporting Information**.

2.5 Statistical procedures

The correlation coefficient between the magnitude of the fission/fusion illusion and the cycle of oscillatory signals was calculated for each electrode position and color coded on a two-dimensional layout of 32 sensors (*r*-maps, **Fig. 3** to **Fig. 6**). **Figure 3B** focuses on the correlation at Oz, because previous studies reported a significant correlation between the alpha cycle and the magnitude of the fission illusion over the occipital cortex (Cecere et al., 2015; Cooke et al., 2019; Keil & Senkowski, 2017). By contrast, in this study there was no a priori assumption regarding brain areas whose oscillatory rhythms were correlated with the fusion illusion. The issue of multiple comparisons was thus resolved by the false discovery rate (FDR) approach (Noguchi & Kubo, 2020; Noguchi, Xia, & Kakigi, 2019), adjusting for the significance threshold using Benjamini-Hochberg correction (Benjamini & Hochberg, 1995). Sensors showing a significant correlation after correction are indicated by black rectangles in **Figure 4** to **Figure 6**.

3. RESULTS

3.1 Behavioral data

Task accuracies in the eight types of trials are shown in **Figure 2A**. A significant difference was observed ($t(28) = 10.91$, $p < 0.001$, Cohen's $d = 2.82$) between 1F0B (95.18 ± 1.03 %, mean ± SE) and 1F2B (39.46 ± 5.08 %), replicating the fission illusion. The fusion illusion was also evident, indexed by a difference ($t(28) = 5.68$, $p < 0.001$, $d = 0.91$) between 2F0B (66.03 ± 4.78 %) and 2F1B (40.33 ± 5.69 %). No significant correlation was observed between the magnitudes of the fission and fusion illusions ($r = -0.19$, $p = 0.31$, **Fig. 2B**).

3.2 EEG data

Figure 3B displays *r*-maps between the magnitude of the fission illusion and the cycles of the six frequency bands from delta to high gamma. Consistent with previous studies, there was a positive correlation between the alpha cycle and the fission illusion at occipital sensors such

as Oz; individuals with a lower alpha frequency showed a larger fission illusion (**Fig. 3C**, right panel).

By contrast, **Figure 4A** shows the magnitude of the fusion illusion correlated with individual beta cycles (lower left panel). Significant correlations after FDR correction (black rectangles) are observed at 16 out of 32 sensor positions. The *r*- and *p*-values at each sensor position, along with the FDR correction procedure, are listed in **Figure S1** (**Supporting Information)**. The *r*-maps between peak frequencies (not central frequencies) and fission/fusion illusions are also provided in **Figure S2**.

Behavioral data indicated that some participants showed low task accuracy (< 50%) in congruent (1F1B and 2F2B) and/or unisensory (1B, 2B, 1F0B, 2F0B) conditions. Furthermore, the scatter plot in **Figure 2B** shows that several participants demonstrated negative illusion magnitudes. An investigation was performed to determine whether the significant correlations in **Figure 4** could be seen even after these participants were excluded from the analysis; the results are shown in **Figure 5**. Correlations between individual beta cycles and the fusion illusion (N = 19) were significant at 25 sensor positions (**Fig. 5D**).

Although I have conducted the correlation analyses using EEG data from -1000 to 0 ms, these waveforms might be contaminated by noises, such as visually-evoked potentials in response to the red fixation point (at -600 to -500 ms, **Fig. 1A**). I thus checked event-related potentials in the pre-stimulus period (**Fig. S3**) and re-analyzed EEG data excluding the noisy period. Correlations between alpha/beta cycles and fission/fusion illusions were kept significant in those analyses.

Recent studies analyzed the magnitude of fission and fusion illusions using measures of signal detection theory (Keil, 2020; Vanes et al., 2016; Watkins et al., 2006), such as perceptual sensitivity (*d'*) and response criteria (ln(β)). I thus computed those measures and correlated each of them with oscillatory cycles. Individual beta cycles were selectively correlated with sensitivity (**Fig. 6A**) but not response bias (**Fig. 6B**) of fusion illusion. Similar results were observed for correlation between alpha cycles and measures of fission illusion (**Fig. S4**).

4. DISCUSSION

In the present study, the magnitudes of the fission and fusion illusions were measured simultaneously in the same group of participants, and the correlations of these magnitudes with neural oscillation cycles in the brain were then examined. The alpha cycle showed a positive correlation with the fission illusion (**Fig. 3**), which replicated the findings of previous

studies (Cecere et al., 2015; Cooke et al., 2019; Keil & Senkowski, 2017; Venskus & Hughes, 2021). In addition, there was a significant correlation between the beta cycle and the fusion illusion (**Fig. 4** to **Fig. 6**).

Several studies have shown a relationship between beta rhythm and audio–visual integration (Ikumi, Torralba, Ruzzoli, & Soto-Faraco, 2019; Kambe, Kakimoto, & Araki, 2015; Michail, Senkowski, Niedeggen, & Keil, 2021; Theves, Chan, Naumer, & Kaiser, 2020; Yuan, Li, Liu, Yuan, & Huang, 2016). For example, strong beta power in the pre-stimulus period predicted the perception of the SIFI in that trial (Kaiser, Senkowski, Busch, Balz, & Keil, 2019; Keil, Muller, Hartmann, & Weisz, 2014). However, most of these studies analyzed the amplitude and phase of beta rhythms rather than their frequency (Cohen, 2014; Lundqvist & Wutz, 2021). The close link between the beta cycle and the fusion illusion in this study provides a new neural measure that can account for inter-individual variation in susceptibility to this illusion.

Why was the length of the beta cycle correlated with the fusion illusion? Although the present data are insufficient to give a complete account, a recent study might help address this issue. In a single group of participants, Cooke et al. (2019) measured inter-individual differences in two types of the double-flash illusion (DFI), one induced by auditory stimuli (beeps) and the other by tactile stimuli (taps on an index finger). While the magnitudes of the auditory DFI were correlated with occipital alpha cycles, the magnitudes of the tactile DFI were positively correlated with individual beta cycles. These results suggest that the human brain has at least two time windows of multisensory interaction, depending on the neural circuits where the interaction takes place. In contrast to the fission illusion, which arises from early interactions (Mishra, Martinez, Sejnowski, & Hillyard, 2007) between primary sensory cortices (Hirst et al., 2020), various brain regions have been reported to be involved in the fusion illusion, including not only unisensory areas (e.g., V1 and A1) but also multisensory areas (e.g., superior temporal sulcus) (Watkins, Shams, Josephs, & Rees, 2007). Furthermore, beta oscillation is thought to play a pivotal role in inter-areal communication between unisensory and multisensory areas (Kayser & Logothetis, 2009; Keil & Senkowski, 2018; Theves et al., 2020). The significant correlations seen in **Figures 4–6** might therefore reflect a relationship between the fusion illusion and a wide neural network across the brain where information is temporally integrated with a beta-band oscillation.

5. CONCLUSION

In addition to demonstrating a significant correlation between individual alpha cycles and the

fission illusion, this study showed a novel correlation between individual beta cycles and the fusion illusion. These results provide further evidence for the separation of neural mechanisms related to the fission and fusion illusions. While a previous study reported the roles of alpha cycles in audio–visual integration and of beta cycles in tactile–visual integration (Cooke et al., 2019), the present data indicate that there are separate time windows for different types of audio–visual integration, one defined by alpha (fission) rhythms and the other by beta (fusion) rhythms.

CONFLICTS OF INTEREST

The author declares no competing financial interest.

ACKNOWLEDGMENTS

This work was supported by KAKENHI Grant Number 19H04430 from the Japan Society for the Promotion of Science (JSPS) to Y.N. I thank Nahomi Sato and Taeko Kaneda for their technical support.

AUTHOR CONTRIBUTIONS

Yasuki Noguchi: conceptualization, formal analysis, investigation, software, visualization, writing of the original draft, and review and editing of the manuscript.

REFERENCES

Abadi, R. V., & Murphy, J. S. (2014). Phenomenology of the sound-induced flash illusion. *Experimental Brain Research, 232*(7), 2207-2220. https://doi.org/10.1007/s00221-014-3912-2

Alais, D., & Burr, D. (2004). The ventriloquist effect results from near-optimal bimodal integration. *Current Biology, 14*(3), 257-262. https://doi.org/10.1016/j.cub.2004.01.029

Andersen, T. S., Tiippana, K., & Sams, M. (2004). Factors influencing audiovisual fission and fusion illusions. *Cognitive Brain Research, 21*(3), 301-308. https://doi.org/10.1016/j.cogbrainres.2004.06.004

Apthorp, D., Alais, D., & Boenke, L. T. (2013). Flash illusions induced by visual, auditory,

and audiovisual stimuli. *Journal of Vision, 13*(5). https://doi.org/10.1167/13.5.3

Bao, V. A., Doobay, V., Mottron, L., Collignon, O., & Bertone, A. (2017). Multisensory Integration of Low-level Information in Autism Spectrum Disorder: Measuring Susceptibility to the Flash-Beep Illusion. *Journal of Autism and Developmental Disorders, 47*(8), 2535-2543. https://doi.org/10.1007/s10803-017-3172-7

Benjamini, Y., & Hochberg, Y. (1995). Controlling the False Discovery Rate - a Practical and Powerful Approach to Multiple Testing. *Journal of the Royal Statistical Society Series B-Statistical Methodology, 57*(1), 289-300. https://doi.org/DOI 10.1111/j.2517-6161.1995.tb02031.x

Bolognini, N., Convento, S., Casati, C., Mancini, F., Brighina, F., & Vallar, G. (2016). Multisensory integration in hemianopia and unilateral spatial neglect: Evidence from the sound induced flash illusion. *Neuropsychologia, 87*, 134-143. https://doi.org/10.1016/j.neuropsychologia.2016.05.015

Brainard, D. H. (1997). The psychophysics toolbox. *Spatial Vision, 10*(4), 433-436. https://doi.org/10.1163/156856897x00357

Cecere, R., Rees, G., & Romei, V. (2015). Individual Differences in Alpha Frequency Drive Crossmodal Illusory Perception. *Current Biology, 25*(2), 231-235. https://doi.org/10.1016/j.cub.2014.11.034

Cohen, M. X. (2014). Fluctuations in Oscillation Frequency Control Spike Timing and Coordinate Neural Networks. *Journal of Neuroscience, 34*(27), 8988-8998. https://doi.org/10.1523/Jneurosci.0261-14.2014

Conrey, B., & Pisoni, D. B. (2006). Auditory-visual speech perception and synchrony detection for speech and nonspeech signals. *Journal of the Acoustical Society of America, 119*(6), 4065-4073. https://doi.org/10.1121/1.2195091

Cooke, J., Poch, C., Gillmeister, H., Costantini, M., & Romei, V. (2019). Oscillatory

Properties of Functional Connections Between Sensory Areas Mediate Cross-Modal Illusory Perception. *Journal of Neuroscience, 39*(29), 5711-5718. https://doi.org/10.1523/Jneurosci.3184-18.2019

DeLoss, D. J., & Andersen, G. J. (2015). Aging, Spatial Disparity, and the Sound-Induced Flash Illusion. *Plos One, 10*(11). https://doi.org/10.1371/journal.pone.0143773

Ernst, M. O., & Bulthoff, H. H. (2004). Merging the senses into a robust percept. *Trends in Cognitive Sciences, 8*(4), 162-169. https://doi.org/10.1016/j.tics.2004.02.002

Faul, F., Erdfelder, E., Lang, A. G., & Buchner, A. (2007). G*Power 3: A flexible statistical power analysis program for the social, behavioral, and biomedical sciences. *Behavior Research Methods, 39*(2), 175-191. https://doi.org/10.3758/Bf03193146

Francisco, A. A., Jesse, A., Groen, M. A., & McQueen, J. M. (2017). A General Audiovisual Temporal Processing Deficit in Adult Readers With Dyslexia. *Journal of Speech Language and Hearing Research, 60*(1), 144-158. https://doi.org/10.1044/2016_Jslhr-H-15-0375

Gogate, L. J., Walker-Andrews, A. S., & Bahrick, L. E. (2001). The intersensory origins of word comprehension: an ecological-dynamic systems view. *Developmental Science, 4*(1), 1-18. https://doi.org/10.1111/1467-7687.00143

Hirst, R. J., McGovern, D. P., Setti, A., Shams, L., & Newell, F. N. (2020). What you see is what you hear: Twenty years of research using the Sound-Induced Flash Illusion. *Neuroscience and Biobehavioral Reviews, 118*, 759-774. https://doi.org/10.1016/j.neubiorev.2020.09.006

Ikumi, N., Torralba, M., Ruzzoli, M., & Soto-Faraco, S. (2019). The phase of pre-stimulus brain oscillations correlates with cross-modal synchrony perception. *European Journal of Neuroscience, 49*(2), 150-164. https://doi.org/10.1111/ejn.14186

Kaganovich, N. (2017). Sensitivity to Audiovisual Temporal Asynchrony in Children With a History of Specific Language Impairment and Their Peers With Typical Development: A

Replication and Follow-Up Study. *Journal of Speech Language and Hearing Research, 60*(8), 2259-2270. https://doi.org/10.1044/2017_Jslhr-L-16-0327

Kaiser, M., Senkowski, D., Busch, N. A., Balz, J., & Keil, J. (2019). Single trial prestimulus oscillations predict perception of the sound-induced flash illusion. *Scientific Reports, 9*. https://doi.org/10.1038/s41598-019-42380-x

Kambe, J., Kakimoto, Y., & Araki, O. (2015). Phase reset affects auditory-visual simultaneity judgment. *Cognitive Neurodynamics, 9*(5), 487-493. https://doi.org/10.1007/s11571-015-9342-4

Kayser, C., & Logothetis, N. K. (2009). Directed Interactions Between Auditory and Superior Temporal Cortices and their Role in Sensory Integration. *Frontiers in Integrative Neuroscience, 3*, 7. https://doi.org/10.3389/neuro.07.007.2009

Keil, J. (2020). Double Flash Illusions: Current Findings and Future Directions. *Frontiers in Neuroscience, 14*. https://doi.org/10.3389/fnins.2020.00298

Keil, J., Muller, N., Hartmann, T., & Weisz, N. (2014). Prestimulus Beta Power and Phase Synchrony Influence the Sound-Induced Flash Illusion. *Cerebral Cortex, 24*(5), 1278-1288. https://doi.org/10.1093/cercor/bhs409

Keil, J., & Senkowski, D. (2017). Individual Alpha Frequency Relates to the Sound-Induced Flash Illusion. *Multisensory Research, 30*(6), 565-578. https://doi.org/10.1163/22134808-00002572

Keil, J., & Senkowski, D. (2018). Neural Oscillations Orchestrate Multisensory Processing. *Neuroscientist, 24*(6), 609-626. https://doi.org/10.1177/1073858418755352

Klimesch, W., Schimke, H., & Pfurtscheller, G. (1993). Alpha frequency, cognitive load and memory performance. *Brain Topography, 5*(3), 241-251. https://doi.org/10.1007/BF01128991

Kostaki, M., & Vatakis, A. (2016). Crossmodal binding rivalry: A "race" for integration

between unequal sensory inputs. *Vision Research, 127*, 165-176. https://doi.org/10.1016/j.visres.2016.08.004

Lewkowicz, D. J., Leo, I., & Simion, F. (2010). Intersensory Perception at Birth: Newborns Match Nonhuman Primate Faces and Voices. *Infancy, 15*(1), 46-60. https://doi.org/10.1111/j.1532-7078.2009.00005.x

Lundqvist, M., & Wutz, A. (2021). New methods for oscillation analyses push new theories of discrete cognition. *Psychophysiology*. https://doi.org/10.1111/psyp.13827

Mahjoory, K., Schoffelen, J. M., Keitel, A., & Gross, J. (2020). The frequency gradient of human resting-state brain oscillations follows cortical hierarchies. *eLife, 9*. https://doi.org/10.7554/eLife.53715

McGovern, D. P., Roudaia, E., Stapleton, J., McGinnity, T. M., & Newell, F. N. (2014). The sound-induced flash illusion reveals dissociable age-related effects in multisensory integration. *Frontiers in Aging Neuroscience, 6*. https://doi.org/10.3389/fnagi.2014.00250

Michail, G., Senkowski, D., Niedeggen, M., & Keil, J. (2021). Memory Load Alters Perception-Related Neural Oscillations during Multisensory Integration. *Journal of Neuroscience, 41*(7), 1505-1515. https://doi.org/10.1523/Jneurosci.1397-20.2020

Mishra, J., Martinez, A., Sejnowski, T. J., & Hillyard, S. A. (2007). Early cross-modal interactions in auditory and visual cortex underlie a sound-induced visual illusion. *Journal of Neuroscience, 27*(15), 4120-4131. https://doi.org/10.1523/Jneurosci.4912-06.2007

Narinesingh, C., Goltz, H. C., & Wong, A. M. F. (2017). Temporal Binding Window of the Sound-Induced Flash Illusion in Amblyopia. *Investigative Ophthalmology & Visual Science, 58*(3), 1442-1448. https://doi.org/10.1167/iovs.16-21258

Noel, J. P., De Niear, M. A., Lazzara, N. S., & Wallace, M. T. (2018). Uncoupling Between Multisensory Temporal Function and Nonverbal Turn-Taking in Autism Spectrum Disorder. *IEEE Transactions on Cognitive and Developmental Systems, 10*(4), 973-982.

https://doi.org/10.1109/Tcds.2017.2778141

Noguchi, Y., & Kubo, S. (2020). Changes in latency of brain rhythms in response to affective information of visual stimuli. *Biological Psychology, 149*. https://doi.org/10.1016/j.biopsycho.2019.107787

Noguchi, Y., Xia, Y., & Kakigi, R. (2019). Desynchronizing to be faster? Perceptual- and attentional-modulation of brain rhythms at the sub-millisecond scale. *Neuroimage, 191*, 225-233. https://doi.org/10.1016/j.neuroimage.2019.02.027

Pelli, D. G. (1997). The VideoToolbox software for visual psychophysics: Transforming numbers into movies. *Spatial Vision, 10*(4), 437-442. https://doi.org/10.1163/156856897x00366

Robertson, D. M. C., & Schweinberger, S. R. (2010). The role of audiovisual asynchrony in person recognition. *Quarterly Journal of Experimental Psychology, 63*(1), 23-30. https://doi.org/10.1080/17470210903144376

Rohe, T., Ehlis, A. C., & Noppeney, U. (2019). The neural dynamics of hierarchical Bayesian causal inference in multisensory perception. *Nature Communications, 10*. https://doi.org/10.1038/s41467-019-09664-2

Samuel, I. B. H., Wang, C., Hu, Z. H., & Ding, M. Z. (2018). The frequency of alpha oscillations: Task-dependent modulation and its functional significance. *Neuroimage, 183*, 897-906. https://doi.org/10.1016/j.neuroimage.2018.08.063

Shams, L., Kamitani, Y., & Shimojo, S. (2000). Illusions - What you see is what you hear. *Nature, 408*(6814), 788-788. https://doi.org/10.1038/35048669

Stevenson, R. A., Segers, M., Ferber, S., Barense, M. D., Camarata, S., & Wallace, M. T. (2016). Keeping Time in the Brain: Autism Spectrum Disorder and Audiovisual Temporal Processing. *Autism Research, 9*(7), 720-738. https://doi.org/10.1002/aur.1566

Tadel, F., Baillet, S., Mosher, J. C., Pantazis, D., & Leahy, R. M. (2011). Brainstorm: A

User-Friendly Application for MEG/EEG Analysis. *Computational Intelligence and Neuroscience, 2011*. https://doi.org/10.1155/2011/879716

Theves, S., Chan, J. S., Naumer, M. J., & Kaiser, J. (2020). Improving audio-visual temporal perception through training enhances beta-band activity. *Neuroimage, 206*. https://doi.org/10.1016/j.neuroimage.2019.116312

Vanes, L. D., White, T. P., Wigton, R. L., Joyce, D., Collier, T., & Shergill, S. S. (2016). Reduced susceptibility to the sound-induced flash fusion illusion in schizophrenia. *Psychiatry Research, 245*, 58-65. https://doi.org/10.1016/j.psychres.2016.08.016

Venskus, A., & Hughes, G. (2021). Individual differences in alpha frequency are associated with the time window of multisensory integration, but not time perception. *Neuropsychologia, 159*. https://doi.org/10.1016/j.neuropsychologia.2021.107919

WalkerAndrews, A. S. (1997). Infants' perception of expressive behaviors: Differentiation of multimodal information. *Psychological Bulletin, 121*(3), 437-456. https://doi.org/10.1037/0033-2909.121.3.437

Wang, A. J., Sang, H. B., He, J. Y., Sava-Segal, C., Tang, X. Y., & Zhang, M. (2019). Effects of Cognitive Expectation on Sound-Induced Flash Illusion. *Perception, 48*(12), 1214-1234. https://doi.org/10.1177/0301006619885796

Watkins, S., Shams, L., Josephs, O., & Rees, G. (2007). Activity in human V1 follows multisensory perception. *Neuroimage, 37*(2), 572-578. https://doi.org/10.1016/j.neuroimage.2007.05.027

Watkins, S., Shams, L., Tanaka, S., Haynes, J. D., & Rees, G. (2006). Sound alters activity in human V1 in association with illusory visual perception. *Neuroimage, 31*(3), 1247-1256. https://doi.org/10.1016/j.neuroimage.2006.01.016

Woynaroski, T. G., Kwakye, L. D., Foss-Feig, J. H., Stevenson, R. A., Stone, W. L., & Wallace, M. T. (2013). Multisensory Speech Perception in Children with Autism Spectrum

Disorders. *Journal of Autism and Developmental Disorders, 43*(12), 2891-2902. https://doi.org/10.1007/s10803-013-1836-5

Yuan, X. Y., Li, H. J., Liu, P. D., Yuan, H., & Huang, X. T. (2016). Pre-stimulus beta and gamma oscillatory power predicts perceived audiovisual simultaneity. *International Journal of Psychophysiology, 107*, 29-36. https://doi.org/10.1016/j.ijpsycho.2016.06.017

Zhou, H. Y., Cheung, E. F. C., & Chan, R. C. K. (2020). Audiovisual temporal integration: Cognitive processing, neural mechanisms, developmental trajectory and potential interventions. *Neuropsychologia, 140*. https://doi.org/10.1016/j.neuropsychologia.2020.107396

Figure captions

Figure 1. Stimuli and task. (**A**) Structure of a single trial. Participants were asked to report the number of flashes (0, 1, or 2) at the end of each trial, neglecting all beeps. The next trial started after a rest screen (300 ms) informing how many trials the participants had completed. (**B**) Sequences of visual and auditory stimuli in a 1-flash & 2-beep (1F2B) trial (left) and a 2F1B trial (right). (**C**) Eight types of trials in which 0–2 flashes were combined with 0–2 beeps. Numbers of trials per experimental session and correct responses (0, 1, or 2) are also shown.

Figure 2. Behavioral results. (**A**) Task accuracies in the eight conditions. Error bars denote standard errors across participants. (**B**) Correlation between magnitudes of the fission and fusion illusions. Each point denotes the data of one participant.

Figure 3. Oscillatory rhythms and the fission illusion. (**A**) The two-dimensional layout of the 32 EEG sensors. (**B**) Correlation *r*-maps between oscillatory cycles and the magnitude of the fission illusion. Black dots and white circles indicate sensors with significant ($p < 0.05$, uncorrected) correlations. (**C**) Scatter plots of individual data points (*x*: alpha cycle, *y*: fission illusion magnitude) at Fz and Oz. *$p < 0.05$.

Figure 4. Oscillatory rhythms and the fusion illusion. (**A**) Correlation *r*-maps between oscillatory cycles and the magnitude of the fission illusion. Sensors with significant correlations after the correction of multiple comparisons are shown by black rectangles. (**B**) Individual data (*x*: beta cycle, *y*: fusion illusion magnitude) at Fz and Oz. Consistent with a previous study (Mahjoory, Schoffelen, Keitel, & Gross, 2020), beta frequencies at an anterior sensor (Fz) were generally higher than those at a posterior sensor (Oz). *$p < 0.05$, **$p < 0.01$

Figure 5. Results of a subgroup of participants (N = 19). Data of participants who showed low task accuracy (< 50%) in congruent (1F1B and 2F2B) or unisensory (1B, 2B, 1F0B, 2F0B) conditions were excluded from the analysis. Data of participants with negative illusion magnitudes were also discarded. Results of the remaining 19 participants are shown in this figure. (**A**) Task accuracies. (**B**) Correlation between magnitudes of the fission and fusion illusions. (**C**) Correlation *r*-maps between individual alpha cycles and magnitudes of the fission illusion. (**D**) Correlation *r*-maps between individual beta cycles and magnitudes of the fusion illusion.

Figure 6. Correlation *r*-maps with measures of the signal detection theory for the fusion illusion. (**A**) Correlations between oscillatory cycles and perceptual sensitivity (*d'*). Participants with lower-frequency beta rhythms showed smaller *d'* values (larger-magnitude fusion illusion). (**B**) Correlations between oscillatory cycles and response criterion ln(β). Positive ln(β) indicates a response bias of reporting "2 flashes" in all types of trials. No significant correlation between oscillatory cycle and ln(β) was observed after FDR correction (black rectangle).

A

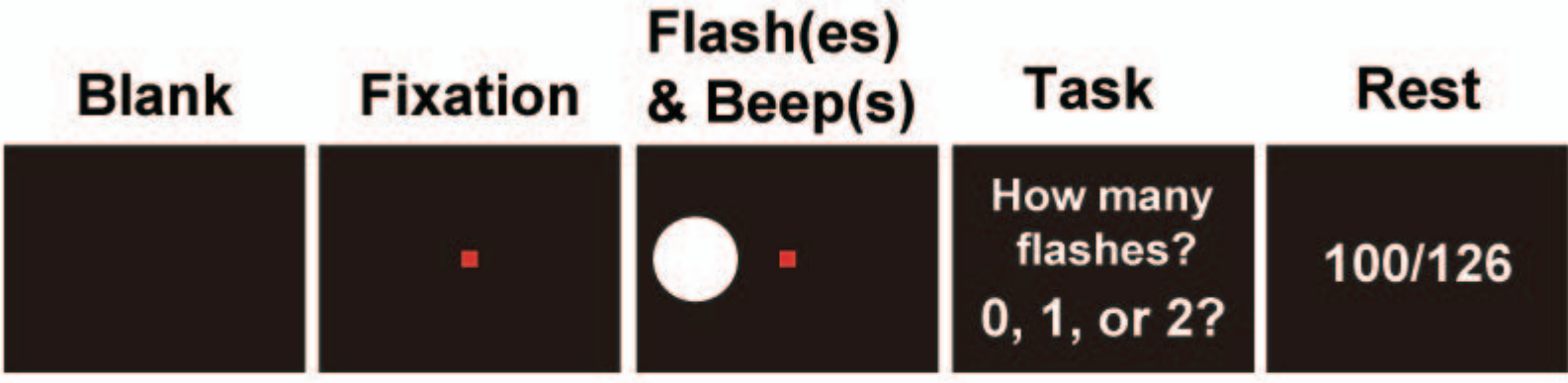

B

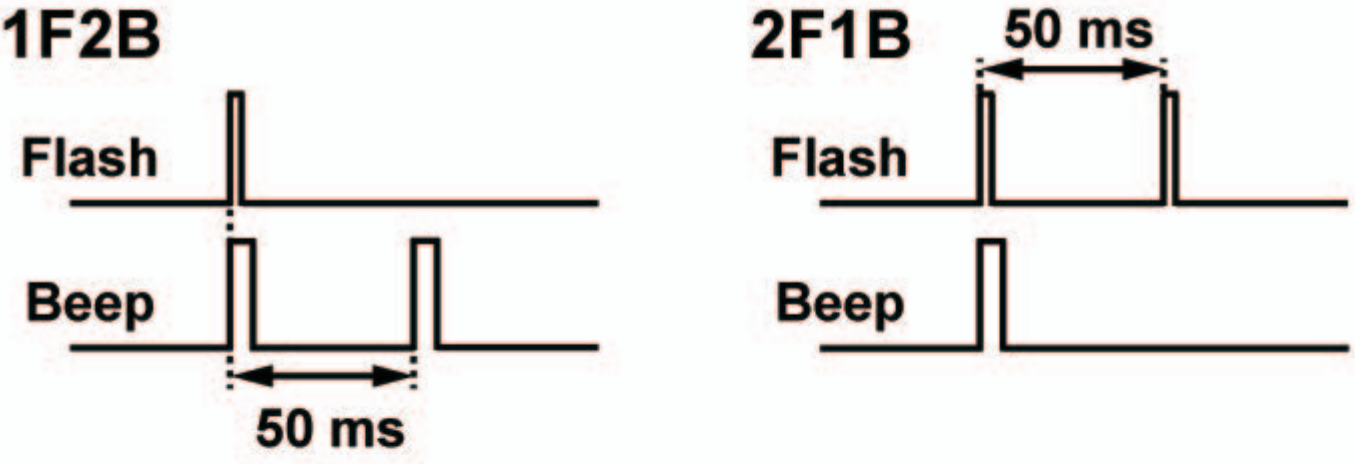

C

	1B	2B	1F0B	1F1B	1F2B (fission)	2F0B	2F1B (fusion)	2F2B
Numers of trials (/session)	9	9	18	18	18	18	18	18
Correct Response	0	0	1	1	1	2	2	2

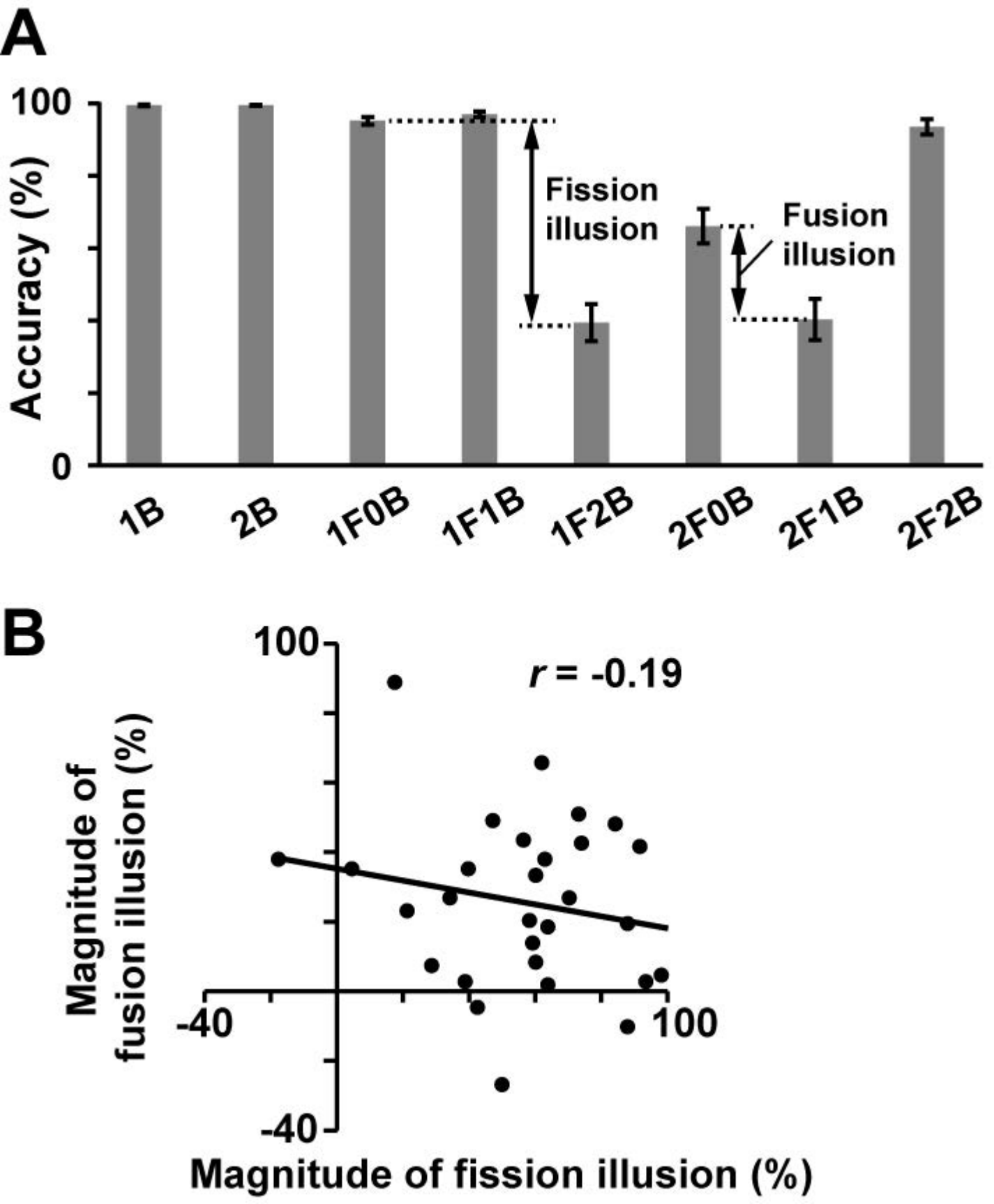
A
100
0
Accuracy (%)
Fission illusion
Fusion illusion
1B
2B
1F0B
1F1B
1F2B
2F0B
2F1B
2F2B
B
100
-40
-40
100
r = -0.19
Magnitude of fusion illusion (%)
Magnitude of fission illusion (%)

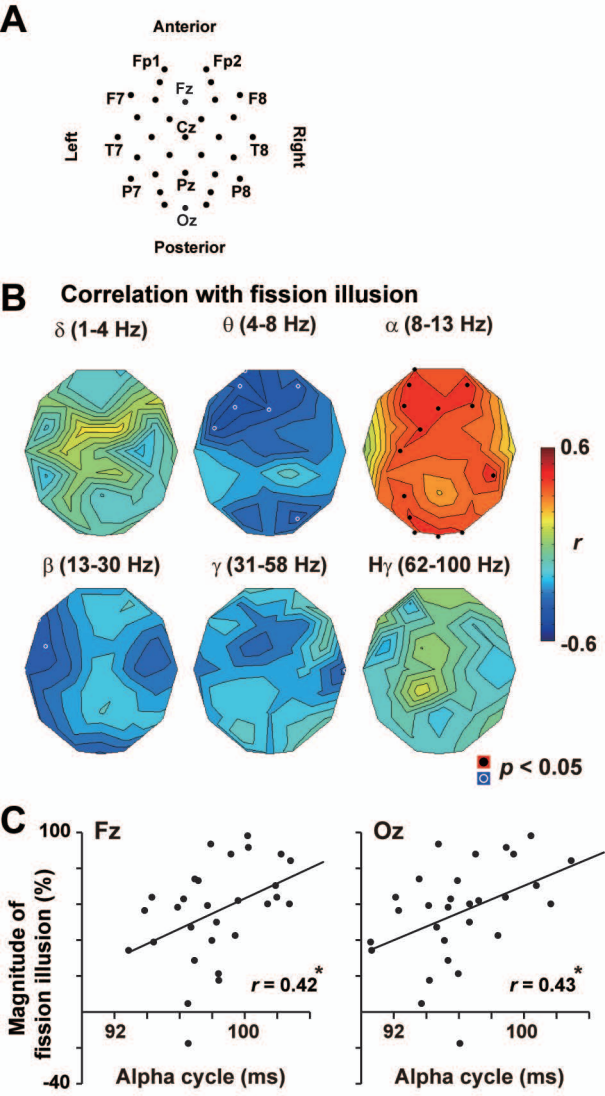
A
Anterior
Fp1
Fp2
Fz
F7
F8
Cz
Left
Right
T7
T8
P7
Pz
P8
Oz
Posterior
B
Correlation with fission illusion
δ (1-4 Hz)
θ (4-8 Hz)
α (8-13 Hz)
β (13-30 Hz)
γ (31-58 Hz)
Hγ (62-100 Hz)
0.6
r
-0.6
p < 0.05
C
Fz
Oz
100
-40
Magnitude of fission illusion (%)
r = 0.42*
r = 0.43*
92
100
Alpha cycle (ms)

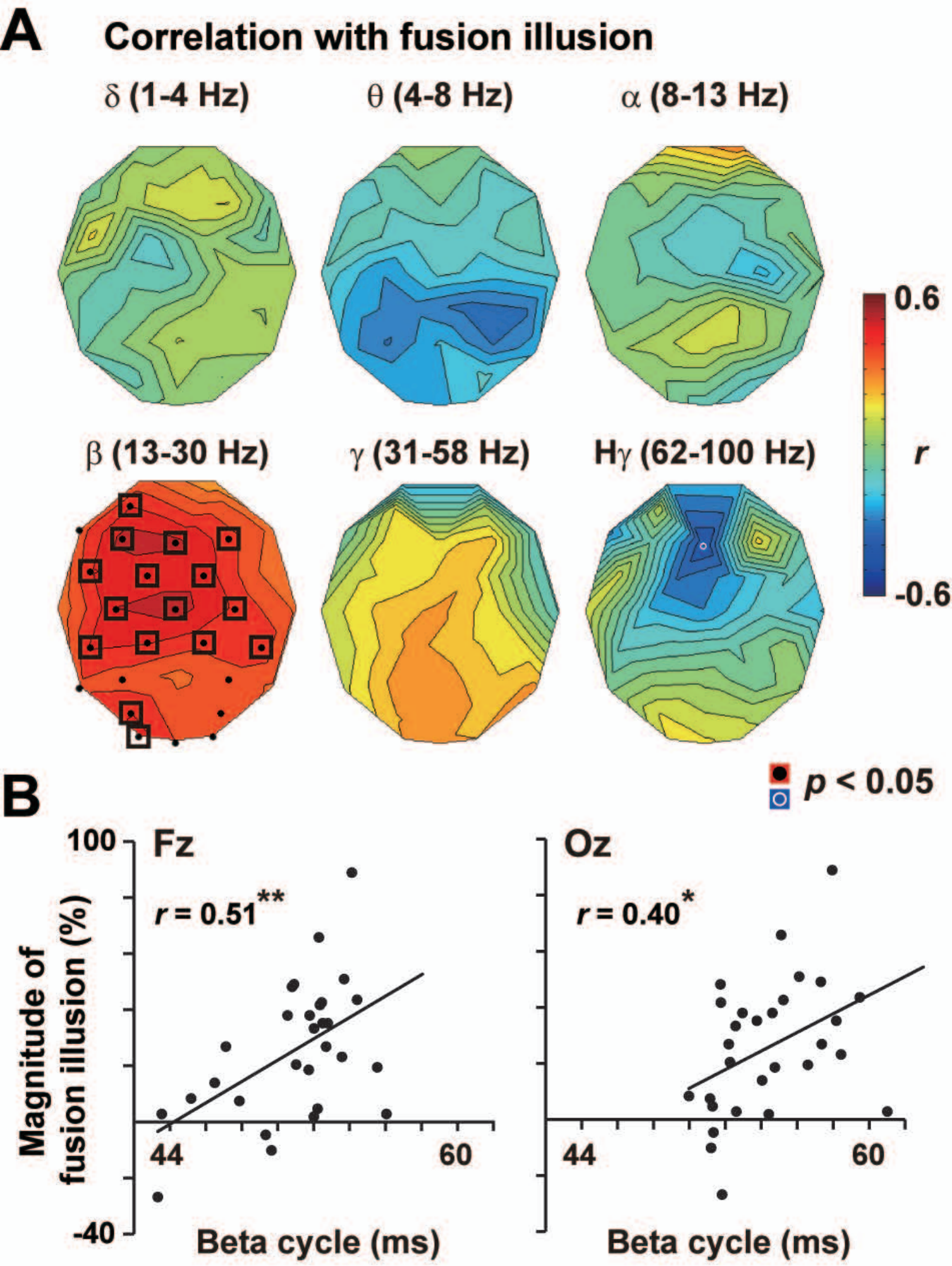
A
Correlation with fusion illusion
δ (1-4 Hz)
θ (4-8 Hz)
α (8-13 Hz)
β (13-30 Hz)
γ (31-58 Hz)
Hγ (62-100 Hz)
0.6
r
-0.6
B
p < 0.05
Fz
r = 0.51**
Oz
r = 0.40*
100
-40
44
60
Magnitude of fusion illusion (%)
Beta cycle (ms)
Beta cycle (ms)

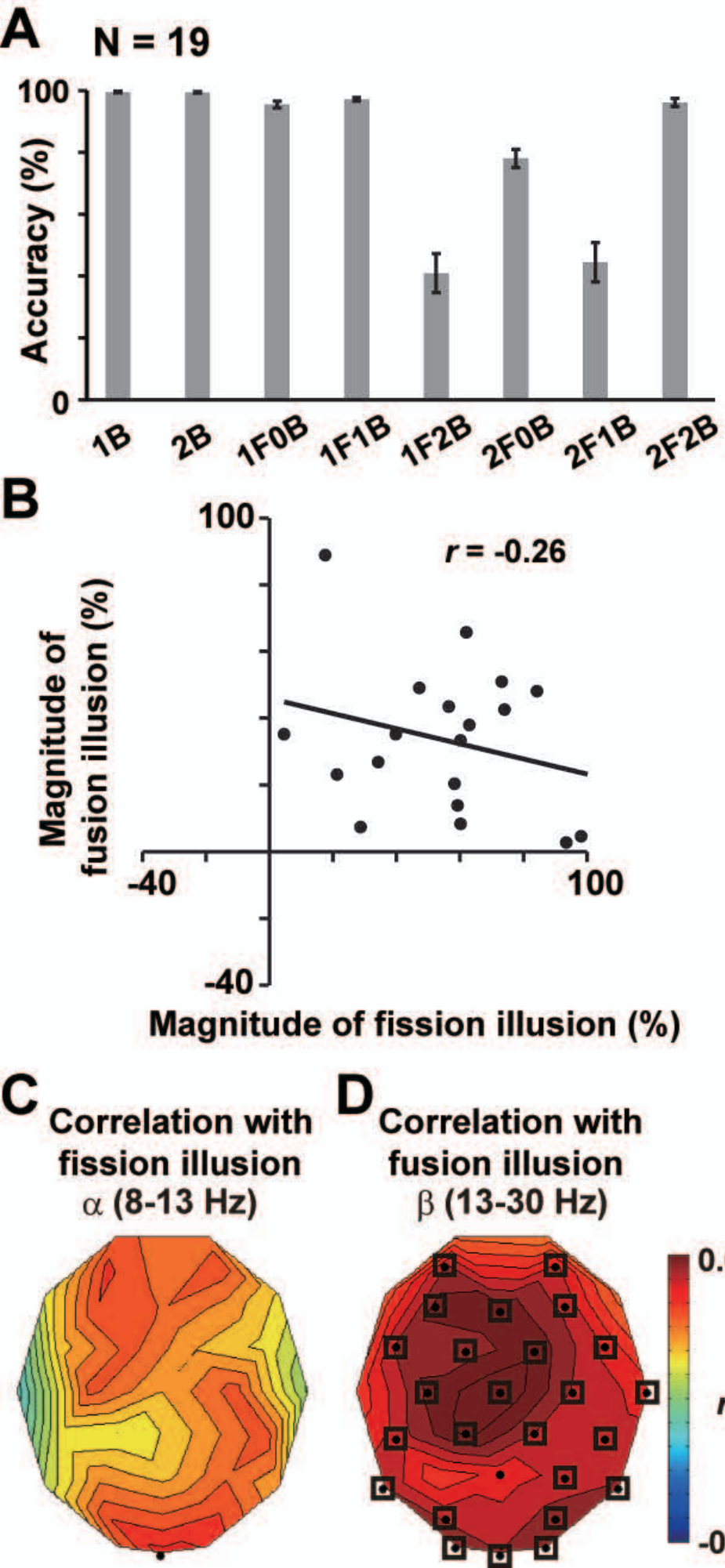
A
N = 19
100
Accuracy (%)
0
1B
2B
1F0B
1F1B
1F2B
2F0B
2F1B
2F2B
B
100
r = -0.26
Magnitude of fusion illusion (%)
-40
100
-40
Magnitude of fission illusion (%)
C
Correlation with fission illusion
α (8-13 Hz)
D
Correlation with fusion illusion
β (13-30 Hz)
0.6
r
-0.6

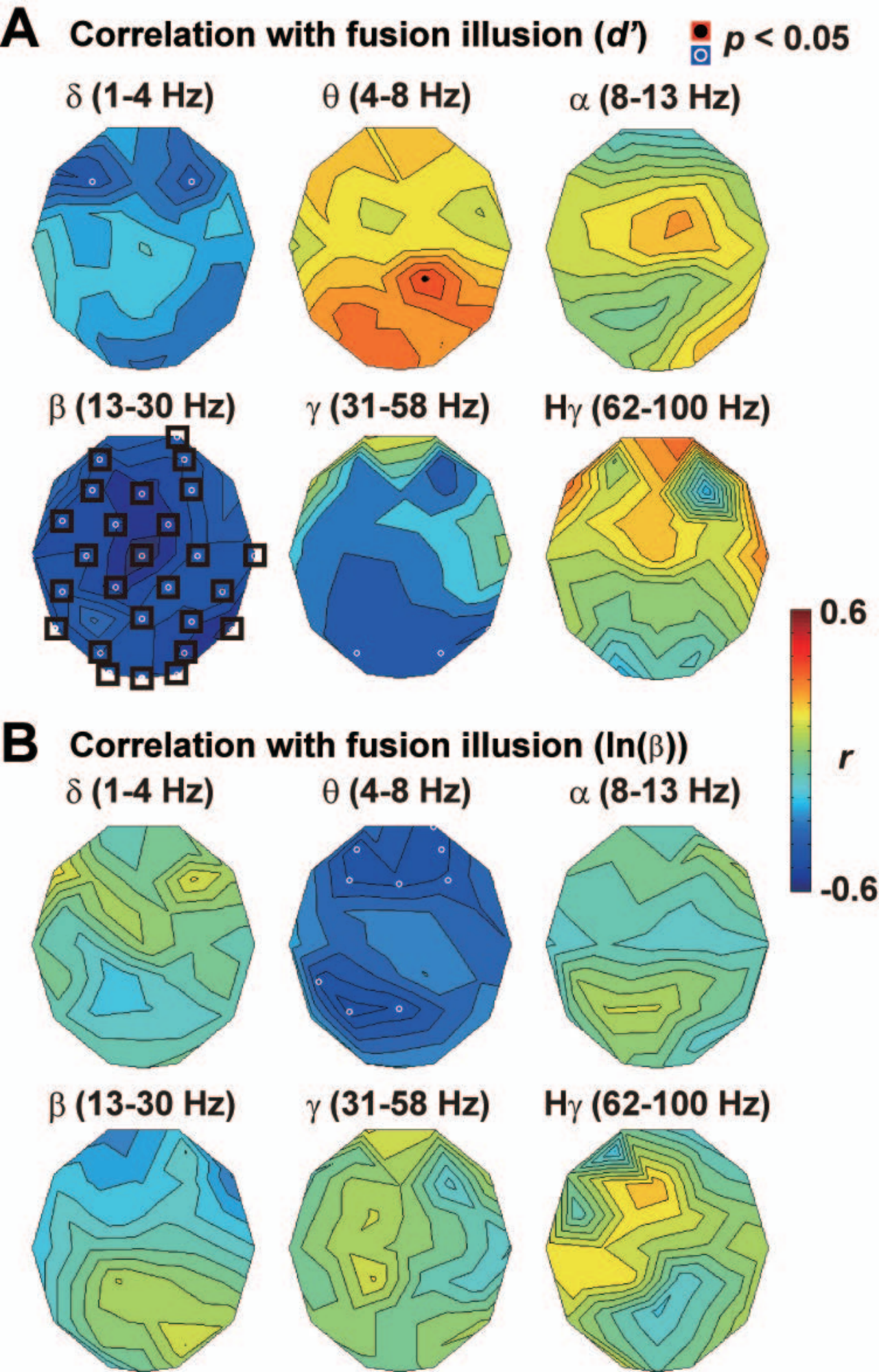
A
Correlation with fusion illusion (d')
p < 0.05
δ (1-4 Hz)
θ (4-8 Hz)
α (8-13 Hz)
β (13-30 Hz)
γ (31-58 Hz)
Hγ (62-100 Hz)
0.6
r
-0.6
B
Correlation with fusion illusion (ln(β))
δ (1-4 Hz)
θ (4-8 Hz)
α (8-13 Hz)
β (13-30 Hz)
γ (31-58 Hz)
Hγ (62-100 Hz)